World Journal of Advanced Engineering Technology and Sciences

eISSN: 2582-8266

Cross Ref DOI: 10.30574/wjaets

Journal homepage: https://wjaets.com/

(RESEARCH ARTICLE)

Check for updates

Analysis on increasing energy efficiency in regional railways by the introduction of permanent magnet synchronous motors

Guilhermo Garcia Burnett *

Department of Electric Energy and Automation Engineering, University of São Paulo, São Paulo, Brazil.

World Journal of Advanced Engineering Technology and Sciences, 2023, 10(01), 001–014

Publication history: Received on 14 June 2023; revised on 25 August 2023; accepted on 28 August 2023

Article DOI: https://doi.org/10.30574/wjaets.2023.10.1.0241

Abstract

Enhancing efficiency has become a fundamental requirement across contemporary technological endeavors aimed at energy conversion. The imperative lies in achieving global energy resource preservation objectives. Novel methods of energy utilization with heightened efficiency are progressively gaining traction, accompanied by the intricacies of refining existing technologies. This research undertakes an examination of the amplified energy efficiency within regional rail systems, achieved through the adoption of permanent magnet synchronous motors (PMSMs) as primary electric propulsion systems, particularly when juxtaposed with induction motors. Delving into the theoretical engineering attributes of PMSMs, coupled with the establishment of dynamic motion characteristics and comprehensive simulations, offers a pathway to amassing empirical insights pertaining to efficiency studies.

Keywords: Drives; Railways; Motors; Efficiency

1. Introduction

In the contemporary progress of technological advancements and energy conversion implementations, like those seen in transportation modes, the emphasis remains on refining efficiency benchmarks to drive cost mitigation and ecological resource preservation. This pursuit is underscored by the integration of environmentally-conscious and electrified technologies, which have accorded prominence to energy efficiency in the realm of transportation. Urban rail networks worldwide underwent electrification several decades ago, establishing themselves as sustainable mobility infrastructures, albeit with notable energy consumption demands. Evolution in traction mechanisms, exemplified by those utilized in railway systems, has exhibited enhancements compared to prevailing technologies like the induction motor and direct current motor. Permanent magnet synchronous motor (PMSM) stands out in the literature as an alternative traction drive on railways, with greater efficiency and power density, absence of rotor losses, smaller volume and ease of control (Cheng et al., 2020) [5]. It is considered the main type of motor capable of competing with the induction machine in railways (Brenna et al., 2018) [3].

PMSM allows direct implementation, without gearboxes, in low-floor vehicles such as trams, which is an advantage that is not possible with induction motors, as they have greater volume (Franko, Kuchta and Buday, 2012) [8]. The permanent magnet synchronous motor also makes it possible to reduce weight, dimensions and costs in railroads, with an increase in the power factor and efficiency, also being able to operate in regenerative braking systems, in addition to being highly applicable in high-speed railroads (Yu et al., 2017) [21]. An improvement in obtaining magnetic alloys has occurred in recent decades, with increased reliability and performance of PMSM in railway traction (Bossio et al., 2020) [2]. This type of machine has, however, some disadvantages, mainly in terms of costs, greater difficulty in protecting against failures, such as demagnetization, vibrations, torque pulsation and higher noise level (Parsa and Toliyat, 2007) [15].

* Corresponding author: Guilhermo Garcia Burnett

Copyright © 2023 Author(s) retain the copyright of this article. This article is published under the terms of the Creative Commons Attribution Liscense 4.0.

A comparative study of energy efficiency is done in this work for the permanent magnet synchronous motor in electric traction, specifically considering the application in regional type railways, mainly in comparison with the consolidated induction motor. The computational railway simulation will allow in this study a reliable acquisition of data about the operation of the PMSM as a traction device in regional railways.

2. Material and methods

PMSM began to show greater applicability in railway electric traction at the end of the 1990s, with the reduction in the cost of obtaining magnetic alloys, and their improvement. The control of this motor was developed specifically for railways at the end of the 20th century (Kondou and Matsuoka, 1997) [14], having high efficiency and high starting torque with high operating speeds. Over the period there was also a qualitative evolution of control methods and semiconductor devices (Edward, Wahsh and Badr, 1998) [7]. The application of induction motors driven by inverters, in combination with gearboxes, consolidated itself as the market standard in terms of electric traction on railways in the early 2000s, with PMSM appearing as a possible alternative, due to its well-known advantages, and the possibility of using it as a direct drive without gearboxes, due to its high torque density, which allows for even greater efficiency due to mass reduction (Frenzke and Piepenbreier, 2004) [9].

Advances in the subject have led to successful introductions of PMSM in railways around the world, such as the commercial operation of the Tokyo subway in 2008, resulting in energy savings, low noise emissions and less complex maintenance, compared to an induction motor of similar power (Shikata et al., 2012) [18]. The permanent magnet synchronous motor was also developed, researched and tested for the use as a traction drive on high-speed railways (Huang et al., 2012) [12].

2.1. Constructive study of PMSM, topologies and materials

Rare earth magnets are a set of materials that represent the main components of the rotor structure of a PMSM. These magnets are mainly composed of NdFeB (known for being expensive and having high sensitivity to higher temperatures), SmCo (even higher cost and lower level of remaining magnetization) (Funieru and Binder, 2008) [10], Alnico (high magnetization capacity, but more susceptible to demagnetization) and ferrite (low-cost ceramic magnetizable material, for complementary use).

The permanent magnet synchronous motor, in constructive terms, is segmented in the literature into the following main topologies, represented in figure 1: SPMSM's (magnets placed on the surface of the rotor) and IPMSM's (magnets positioned inside the rotor), which have “U” and “V” subtypes (Duan, Ou and Deng, 2020) [6]. The internal magnet motor produces hybrid torque by both the magnetic and reluctance torque components (caused by the saliences), resulting in superior response and higher power density. The surface magnet machine, in turn, presents greater losses due to eddy currents (at high speeds), requiring the insertion of belts to retain the magnets.

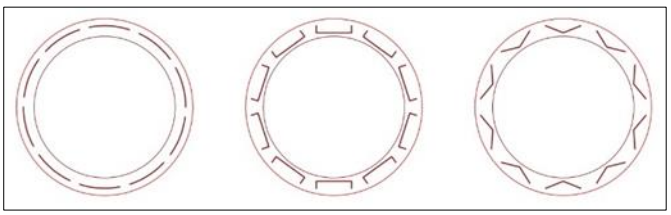

Figure 1 Rotor structures for SPMSM, IPMSM “U” and IPMSM “V”

For an optimized magnetic direction of the PMSM, flux barriers can be introduced, in favor of increasing the saliency and the reluctance torque, also reducing the flux dispersion. The PMSM stator can be configured with concentrated windings (applicable to the SPMSM, with less salience, compromising the torque reluctance in the case of the IPMSM) or distributed (Vagati, 2012) [19].

2.2. Magnetic, circuit analysis and modelling of PMSM

Analogously to what is known for the conventional three-phase synchronous machine, a rotating field is established in the PMSM air gap from three stator windings spaced by 120 electrical degrees. In the rotor, the field windings are replaced by the fixed excitation provided by the permanent magnets. Torque is developed only at synchronous speed, requiring variable frequency starting and control techniques. The losses in this machine occur in the stator copper, in the iron, in addition to supplementary and mechanical losses (Chapman, 2011) [4]. The magnetic flux density in PMSM

does not present precision when analyzed by the magnetic equivalent circuit, being necessary the study by the computational finite element method (FEM). Equation (1) is simplified to the per-phase equivalent circuit of the stator of a non-salient PMSM, with the terminal voltage U presented as a function of the values of resistance R, current I, inductance L and induced voltage Ui. Figure 2 shows simplified circuit by phase of the machine's stator and phasor diagram.

$$U = RI + j\omega LI + U_i \dots\dots\dots\dots (1)$$

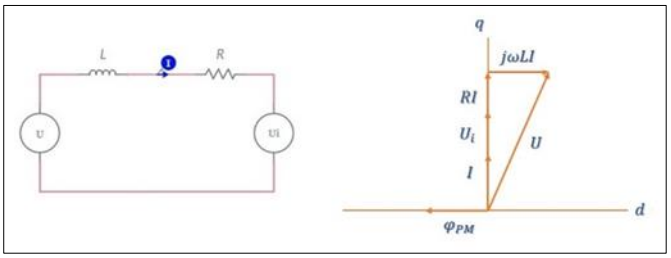

Figure 2 Simplified PMSM stator per-phase circuit and phasor diagram

It is possible to model the magnetic dynamics of operation of the PMSM both in the stationary reference "αβ" and through the "dq" coordinate system of rotating axes, through equations (2) and (3), in terms of currents, voltages, resistances and direct and quadrature axis stator inductances, in addition to the angular frequency ω, direct axis stator magnetic flux φSd and quadrature axis stator magnetic flux φSq.

$$U_{Sd} = R_S I_{Sd} + L_{Sd}\frac{dI_{Sd}}{dt} - \omega\varphi_{Sq} \dots\dots\dots (2)$$

$$U_{Sq} = R_S I_{Sq} + L_{Sq}\frac{dI_{Sq}}{dt} - \omega\varphi_{Sd} \dots\dots\dots (3)$$

Torque Te, is evaluated by equation (4) as a function of the number of poles p, magnetic flux of the permanent magnets φPM, currents and inductances of the direct and quadrature axes, and is composed of a magnetic component and a reluctance component, with the direct axis inductance LSd and quadrature axis inductance LSq being equivalent in SPMSM, with only the presence of the reluctance component.

$$T_e = \frac{3}{2}\frac{p}{2}\left(\varphi_{PM} I_{Sq} + \left(L_{Sd} - L_{Sq}\right) I_{Sd} I_{Sq}\right) \dots\dots (4)$$

2.3. Analysis of PMSM Control and protection methods

The two main methods used for PMSM control are (Brenna et al., 2018) [3]: vector field-oriented control (FOC), combined with individual pulse width modulation (PWM), and the direct torque control (DTC) technique. The FOC strategy, similarly to direct current machines control, is based on a decoupling of the stator current in components associated with torque and flux, in terms of the direct and quadrature axes, respectively, through the Park's "dq" referential transform and use of proportional integral (PI) controllers. In Figure 3 is shown an example of a field-oriented control diagram for permanent magnet synchronous motor.

The DTC strategy, as an alternative, is based on direct flux and torque control for the PMSM, through the use of non-linear hysteresis controllers. The direct torque control method makes it possible to generate a sinusoidal flux in the stator without the need for reference transformations to obtain decoupled control between flux and torque. The DTC method also does not require the use of PWM modulators, as the control is composed of switching tables dependent on the outputs of the hysteresis controllers, based on spatial vector modulation (SVM) in the "αβ" stationary two-phase reference. Selection of voltage vectors makes it possible to control the flux path speed of the machine.

Considering constant magnitudes of the PMSM IS stator current, the electromagnetic torque becomes a function of the angle θ between the current and the direct axis "d". The control method based on maximum torque per ampere (MTPA) estimates the ideal angle θ that produces the highest possible torque for a given current value.

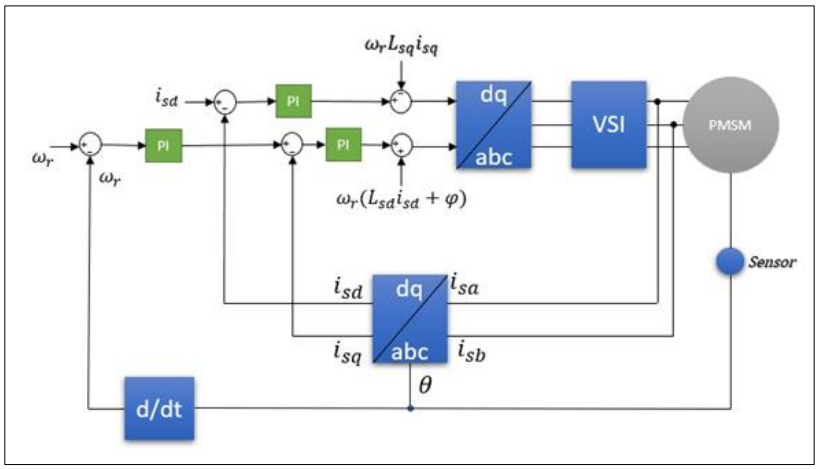

Figure 3 Control of PMSM with FOC method

The possible defects during the operation of a permanent magnet synchronous motor are associated with stator faults, rotor faults, bearing problems and inverter defects. Costs are generated as a consequence of failures, with the need for maintenance stops and the time the traction machine remains inoperative (Bossio et al., 2020) [2]. The traction PMSM is susceptible to demagnetization and insulation failures at high temperatures, so thermal analysis is of high importance in the design of the machine, in search for having a correct dimensioning of the cooling system and insulation classes. Methods seen in state-of-the-art for permanent magnet synchronous motor protection are based on mathematical tools, together with data processing techniques collected by torque, current and voltage sensors, allowing the detection of abnormal conditions.

A point of difficulty is the temperature detection of the magnets coupled to the PMSM, since the rotor is a moving part. Methods for direct temperature detection of magnets can be based on contact sensors, such as resistors and thermocouples, or on non-contact infrared sensors. Detection methods involving contact, although more accurate and easier to obtain, require sensors and data transmission devices and, therefore, imply higher costs and lower control robustness.

In recent years the development of machines with higher fault tolerance capacity (fault-tolerant machines) has intensified, also with the PMSM, in which the introduction of redundant systems makes it possible to reduce probabilities of failure. The design of multiphase permanent magnet synchronous motors stands out, with a number of isolated and independent phases greater than three, as the three-phase dual powered configuration (DTP-PMSM) (Xu et al., 2020) [20].

2.4. PMSM and Classic Drives Comparison in Electric Traction

The DC motor was popularized in variable speed electric traction before the induction motor and PMSM, having attributes of low cost and ease of control through switched power converters. Although the direct current motor was flexible for operation in terms of connection topologies for the excitation circuits, like the variable speed series topology for traction, the presence of the collector-brush mechanism is a disadvantage, related to the occurrence of wear by mechanical friction. The DC traction motors were also designed to operate in generator mode with regenerative braking, converting kinetic energy into electrical energy during periods of reduced speed, in addition to operating under field weakening, allowing operation at speeds above the nominal, with reduced torque. The induction machine subsequently emerged as the predominant standard for electric traction (including rail) in recent decades, due to its greater constructive resistance, lower cost and high applicability for operation at variable speed.

The cost of an electric machine is dependent on some market variables, and in the permanent magnet synchronous motor, the presence of permanent magnets implies higher production costs, in addition to the need to apply an exclusive inverter for the control of each PMSM. The cost reduction strategies for this machine are based, for example, on the geometric modification of the topology of the magnets, in addition to the use of sensorless control methods, reducing construction costs by reducing the number of installed sensors.

In order to make it possible to replace induction motors with permanent magnet synchronous machines on railways, considerable investments are required, considering the necessary adaptations. For the upgrade to be economically

viable, the amount spent must be recovered in an acceptable period of time. Traction drives suitable for rail vehicles must meet the requirements of robustness, durability, alignment with weight characteristics, vibrations, reduced noise, easy maintenance and high efficiency. Alternating current motors (induction and permanent magnet synchronous) were consolidated in railway traction, replacing direct current motors, due to the less intensive maintenance regime combined with greater power density and greater reliability.

The permanent magnet synchronous motor is a potential alternative to the induction motor in applications such as electric railway traction, with typical theoretical efficiency between 95% and 97% (compared to values between 93% and 95% for the induction motor) (Koerner, Cai and Adam, 2017) [13]. PMSM can contribute to increasing energy efficiency in railways, reducing losses, and also through the use of regenerative braking techniques and application of control methods based on maximum torque per ampere.

2.5. Movement Dynamics in Railways

The dynamics of movement on railways is studied by analyzing the temporal and spatial locomotion of the vehicles, in three-dimensional terms of the longitudinal, transverse and vertical directions, having kinematic variables such as: speed, displacement, acceleration and jerk, the variation of acceleration in time. The movement can be diversified between rotation, oscillation and translation, depending on the technical characteristics of the railways in relation to curves and ramps.

Railway electric traction is based on the set of electric drives and the complex mechanics of traction loads. The friction between the wheels and the rail allows the torque produced by the motors to be transferred to the wheels in the form of force, pushing the train through a mechanism called adhesion, whose force Fa is shown by equation (5), as a function of the coefficient of adherence μ and the normal reaction force N, being a property in which the wheel exerts a maximum tractive motor effort on the rails, maintaining contact without slipping.

$$F_a = \mu N \ldots\ldots\ldots\ldots (5)$$

A simplified model of the dynamics of a train in a traction system can be presented by a differential equation represented by equation (6), in terms of the mass M and resistance effort RM to the movement of the train, tractive effort FM and speed V (Halder, Agarwal and Srivastava, 2015) [11].

$$M\frac{dV}{dt} = F_M - R_M - Mgsen\theta \ldots\ldots\ldots (6)$$

The tractive motor effort can be increased until reaching the limit of adhesion during the movement of a railway vehicle, moment from which the wheel starts to slip (Brenna et al., 2018) [3]. The natural grip is based on the reversible and combined effect of microslips and elastic deformations, being a condition present even in braking situations. The coefficient of adhesion is a function of parameters such as speed and interface characteristics between the wheels and their respective contact surfaces, occurring between experimental values from 0.15 to 0.85, in relation to the materials involved and rails in wet or dry conditions. In railway vehicles, the traction effort is transmitted through several mechanical interfaces until it is applied to the wheels, so that each vehicle is formed by wheel sets (pairs of wheels interconnected by an axle) and bogies. Figure 4 shows the main forces present in a train wheel.

Total resistance to motion Rm is a composition of resisting forces acting in opposition to the motion of the train, in terms of the normal resistance to displacement R0, the resistance due to rolling R1, sum of the resistance R'1 due to the mechanical shaft-bearing interface and the resistance R''1 related to the wheel-contact surface interface, and the air resistance R2; and the combined supplementary resistance Re, respectively the sum of the resistance Ri due to ramps and Rc due to curves. The following relations are presented in equations (7), (8) and (9).

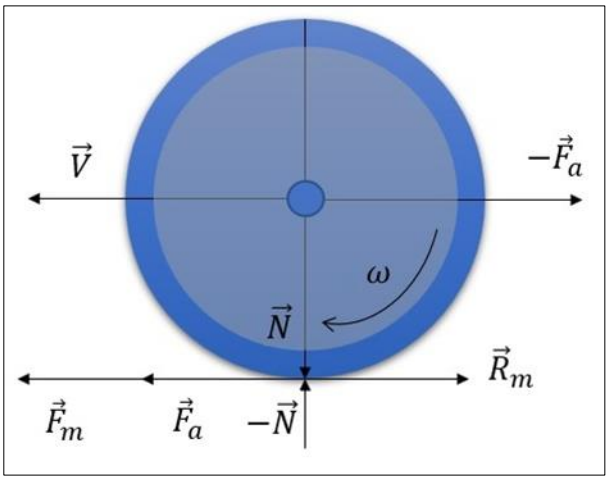

Figure 4 Forces acting on a train wheel

$$R_m = R_0 + R_e \dots\dots\dots\dots (7)$$

$$R_0 = R_1 + R_2 = R'_1 + R''_1 + R_2 \dots\dots\dots\dots (8)$$

$$R_e = R_i + R_c \dots\dots . (9)$$

An alternative way of presenting the normal resistance to motion is provided by the equation (10), known as Davis formula, dependent on velocity V, and parameters related with the mechanical resistances of rolling and friction (respectively coefficients A and B) and air (coefficient C).

$$R_0 = A + BV + CV^2 \dots\dots\dots .. (10)$$

The point-by-point study of the kinematic and electrical characteristics of railway traction systems can be done by using railway computational simulation, a modeling tool based on geometric data of tracks and lines, such as curves, ramps, extensions and stations, in addition to parameters of rail vehicles, such as tractive effort, mass and drive properties. The railway simulation allows the calculation and prediction of the performance of trains in a specific railway route, in order to enable the project of the electric traction system, providing train results, such as speed, position, acceleration, travel time, tractive effort, current and power demanded.

In recent decades, most of the developed traction permanent magnet synchronous motors have rated power units ranging from 150kW to 2500kW, with maximum torque between 1500Nm and 13500Nm (Koerner, Cai and Adam, 2017) [13].

In order to preserve the mechanical braking devices and maximize energy efficiency in railways, regenerative braking must be provided by the PMSM from the lowest speeds (Kondou and Matsuoka, 1997) [14]. Dynamic braking complements mechanical friction braking, based on the transformation of kinetic energy from train braking into electrical energy internally to the traction motors, which is then dissipated by means of resistors. Regenerative braking, in turn, transfers the recovered energy to receptive contact lines so that it can be stored in batteries for later use or consumed by other trains.

2.6. Case Study

In this work, in the form of a case study, a comparison will be made between the use of the permanent magnet synchronous motor as an alternative to the induction motor in a future Brazilian urban regional railway line, the Intercity Train North Axis, of the state of São Paulo. The operation of the Intercity Train will meet the demands of express and stop services, connecting a length of 101 km between the cities of São Paulo, Jundiaí and Campinas, with an estimated travel time of approximately 1 hour at rush hours (Metropolitan Transportation Authority, 2021) [17]. The electric trains on this railway are expected to reach a maximum speed of up to 140km/h with high levels of acceleration, transporting up to eight hundred passengers. The case study will provide results, through railway computational simulation, which will provide data to be analyzed and processed, in order to obtain conclusions about levels of energy

efficiency, efforts involved, power developed, energy savings and consumption, depending on variables such as displacement and speed of trains on the railway line.

Variables associated with the technical aspects of the railway under study will be provided to the railway simulation software, also in terms of train characteristics and traction drives, and through the train's Davis formula. The simulation will make it possible to draw conclusions about the energy efficiency levels of the permanent magnet synchronous motor in relation to the induction motor, depending on the characteristics of the train and railway network under study. For the case study, the train model considered will consist of a locomotive exclusively dedicated to electric traction, without having a passenger hall, coupled to six double-decker cars without their own traction. The traction locomotive will be technically inspired by the ALP-46 model, while the passenger cars will be inspired by the MultiLevel Coach, both publicly known for being utilized in the New Jersey Rail System. Tables 1 and 2 below show the main technical characteristics of the ALP-46 locomotive and the MultiLevel Coach wagon.

Table 1 ALP-46 locomotive specifications

Technical Specification	Value
Mass	90000kg
Power	5300kW
Braking Effort	150kN
Length	19.56m
Width	2.95m
Height	4.47m

Table 2 MultiLevel Coach Car Specifications

Technical Specification	Value
Mass	60323kg
Length	25.91m
Width	3.05m
Height	4.42m

The acceleration of the trains must not be less than $0.7 m/s^2$, under nominal load condition with straight level tracks. Final acceleration under maximum operating speed should be a minimum of $0.25 m/s^2$, and at any speed the jerk should not be greater than $0.6 m/s^3$.

3. Results and discussion

From equations (11), (12), (13) and (14) it is possible to numerically obtain coefficients of the Davis formula for the locomotive and wagons used as a model for the case study, at first considering the application of induction motors. The coefficients will be transformed from specific values, in N/kN, to absolute values, in N, by multiplying by the weight in kN of each vehicle. Table 3 shows the Davis formula coefficients for the train model, so that each train parameter is formed by the sum of the respective parameter associated with the locomotive with six parameters of the wagon model. mev represents the average mass per axle of the vehicle, while mv represents the average mass of the vehicle and sv the frontal section area of the vehicle.

$$A_{locomotive} = A_{car} = 0.65 + \frac{13.15}{m_{ev}} \left[\frac{N}{kN}\right] \ldots\ldots\ldots (11)$$

$$B_{locomotive} = B_{car} = 0.00932 \left[\frac{N \text{ x } h}{kN \text{ x } km}\right] \ldots\ldots\ldots (12)$$

$$C_{locomotive} = 0.00456\left(\frac{s_v}{m_v}\right)\left[\frac{N \text{ x } h^2}{kN \text{ x } km^2}\right] \ldots\ldots\ldots (13)$$

$$C_{car} = 0.000645\left(\frac{s_v}{m_v}\right)\left[\frac{N \text{ x } h^2}{kN \text{ x } km^2}\right] \ldots\ldots\ldots (14)$$

Table 3 Coefficients for case study train model Davis formula considering use of induction motors

Coefficient	Value
A [N]	6487.20506
B [N x h/km]	41.27820917
C [N x h²/km²]	1.100558718

The resulting equation (15) will allow obtaining the tractive motor effort curve as a function of speed for the train, formed by a locomotive coupled to six wagons, which in total sum up to 451.938 tons of mass, either in the acceleration or braking regimes, from the nominal acceleration of 0.7m/s².

$$F_m - (R_0 + R_i + R_c) = m' \; x \; a \ldots\ldots (15)$$

Two regions characterize the curve, constant tractive effort and constant power. The calculation of the constant tractive effort will be done considering zero speed and nominal acceleration, while the constant power will come from the mechanical power supplied by the motors. The ramps and curves are variable along the railway, therefore the respective related resistances will be considered zero value. The term R0 will be equivalent to the coefficient A of the train's Davis formula, since zero speed was adopted. Below, equation (16) is presented, in which the inertia mass m' of the train is equal to the multiplication of the inertia factor ξ of the rotating masses (respectively with an average value of 1.1 for a complete train) by the mass of the train m:

$$F_m = A + m' \; x \; a \ldots\ldots\ldots\ldots (16)$$

Expression (16), subsequently developed numerically through expressions (17), (18) and (19), allows obtaining the value of the tractive effort in the constant region.

$$F_m = 6.48720506 + 451.938 \; x \; 1.1 \; x \; 0.7 \ldots\ldots\ldots\ldots (17)$$

$$F_m = 6.48720506 + 347.99226 \ldots\ldots\ldots\ldots (18)$$

$$F_m = 354.4794651 \; [kN] \ldots\ldots\ldots (19)$$

In the constant power region, the traction effort FM is obtained through expression (20), developed numerically by equations (21) and (22), as a function of the speed V of the train and the total power P delivered by the locomotive engines, having the shape of a hyperbola.

$$F_m = \frac{P \; x \; 3.6}{V} \ldots\ldots\ldots\ldots (20)$$

$$F_m = \frac{5300 \; x \; 3.6}{V} \ldots\ldots\ldots\ldots (21)$$

$$F_m = \frac{19080}{V} [kN] \ldots\ldots\ldots\ldots (22)$$

The acceleration of the train at maximum speed must be at least 0.25 m/s², therefore a third curve will be introduced, the reduced power region, to be obtained by calculating the motor effort Fm' evaluated now for the minimum acceleration and the maximum speed Vmax 140km/h. At this point, however, the effort will represent a $1/V^2$ type ratio, instead of 1/V (constant power). Also based on equation (16), for this condition below is the development of expressions (23), (24), (25) and (26).

$$F_{m\prime} = A + BV + CV^2 + m'x\ a \ldots\ldots\ldots\ldots\ldots\ldots (23)$$

$$F_{m\prime} = 6.48720506 + 0.04127820917V + \cdots$$
$$\ldots\ 0.00110055871V^2 + 451.938\ x\ 1.1\ x\ 0.25 \ldots\ldots\ldots\ldots (24)$$

$$F_{m\prime} = 6.48720506 + 0.04127820917(140) + \cdots$$
$$\ldots 0.00110055871(140^2) + 124.28295$$
$$\ldots\ldots\ldots\ldots (25)$$

$$F_{m'} = 158.1200551\ [kN] \ldots\ldots\ldots\ldots\ldots (26)$$

Tractive effort curve in the reduced power region is provided by equation (27), developed numerically in expressions (28) and (29).

$$F_m = \frac{F_{m\,\prime}\ x\ {V_{max}}^2}{V^2} \ldots\ldots\ldots\ldots\ldots\ldots\ldots (27)$$

$$F_m = \frac{158.1200551\ x\ (140)^2}{V^2} \ldots\ldots\ldots\ldots\ldots (28)$$

$$F_m = \frac{3099153.079}{V^2}[kN] \ldots\ldots\ldots\ldots (29)$$

Figure 5 shows the graph of tractive effort as a function of speed for the case study train, considering the use of induction motors, containing the regions of constant effort, constant power and reduced power, with the comparison in the background with the train's Davis formula.

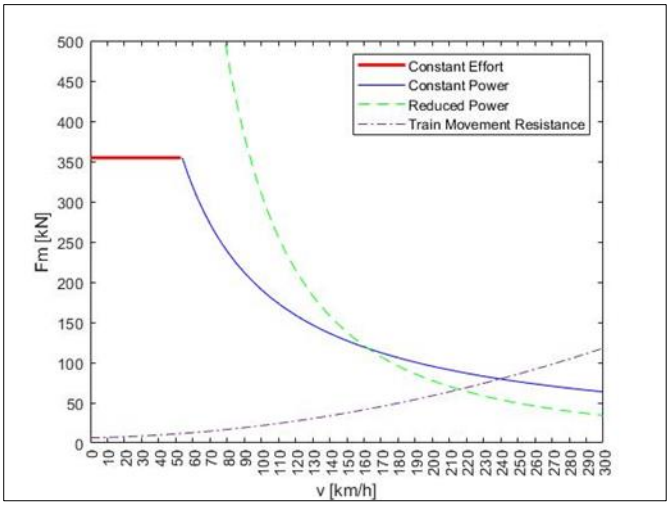

Figure 5 Movement resistance and tractive effort curves as a function of speed for the case study train with application of induction motors

The curves of tractive effort and movement resistance as a function of speed for the case study train will now be obtained considering the use of PMSM's, as shown in figure 6. The curves will make it evident, in a practical way, the advantage of the lower mass of the PMSM for the same total power of 5300kW of the locomotive, divided between four machines of 1325kW each, in relation to the induction motor.

Each permanent magnet synchronous motor of the case study locomotive will have a proper value of applied mass of 1152 kg, which is introduced after subtracting the mass of 1472 kg of each induction motor from the total mass of the locomotive. Obtaining the mass of the motors was carried out using the theoretical power density ratios, respectively 0.9kW/kg for the induction motor and 1.15kW/kg for the PMSM. After applying the PMSM's, the locomotive's mass was reduced to 88.720 tons, which added to the masses of six wagons of 60.323 tons each, represents the total mass of 450.658 tons for the train. In this way, a total reduction of 1280kg was achieved compared to the previous train with

induction motors. Table 4 shows the Davis formula coefficients for the case study train model considering the use of permanent magnet synchronous motors.

Table 4 Davis formula coefficients for case study train model considering use of PMSM's

Coefficient	Value
A [N]	6479.05146
B [N x h/km]	41.16129909
C [N x h^2/km^2]	1.100558718

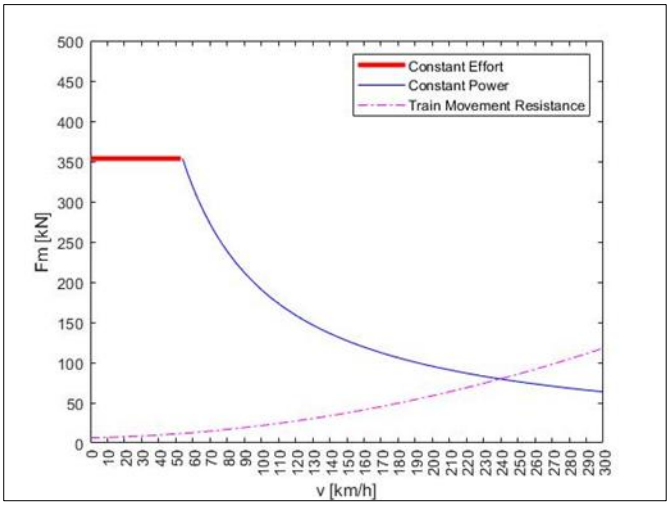

Figure 6 Movement resistance and tractive effort curves as a function of speed for the train of the case study with PMSM's

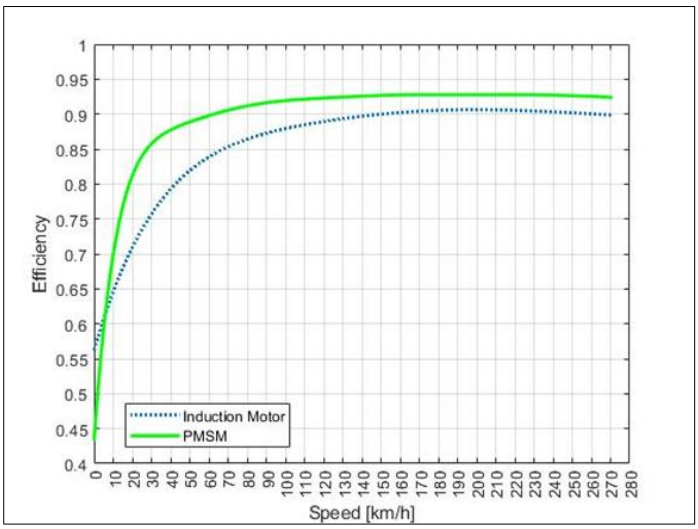

Figure 7 Efficiency as a function of speed for induction motor and permanent magnet synchronous motors considered in the case study

Figure 7 shows efficiency percentage curves as a function of train speed (km/h) for the induction motor and permanent magnet synchronous motor models adopted in the case study simulations. The indices were obtained inspired by (Sandberg, 2010) [16]. An efficiency of 98% was considered for the transmission mechanisms, to compose the overall efficiency of the train, in addition to an efficiency of 98% for the electronic drive. The speed values were transformed from rpm to km/h by means of the wheel diameter of the ALP-46 locomotive, of 1118mm, and also by the transmission

ratio of 1:3.714 (Allenbach, 2016) [1] from the ALP-45 locomotive, similar to locomotive model adopted in the case study.

The case study of this work is made possible by computational railway simulations, through the introduction of previously calculated variables, in order to obtain data and examples of representative curves of the dynamic behavior of trains, whether equipped with induction motors or PMSM's, on the analyzed railroad, which has stop stations in Barra Funda, Jundiaí and Campinas, with train traffic in both directions. Figure 8 shows as an example the temporal variation of speed for the case study train, on the Campinas – Barra Funda route with the application of induction motors.

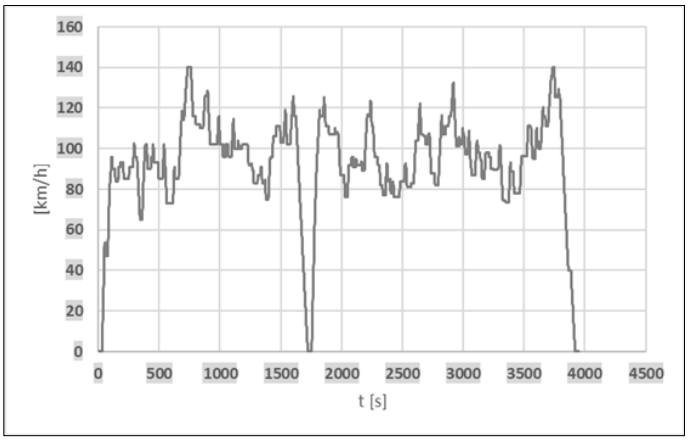

Figure 8 Temporal variation of speed for train of the case study, Campinas – Barra Funda route with induction motors

Figure 9 shows tractive effort as a function of time for the train of the case study, Campinas – Barra Funda route using PMSM's.

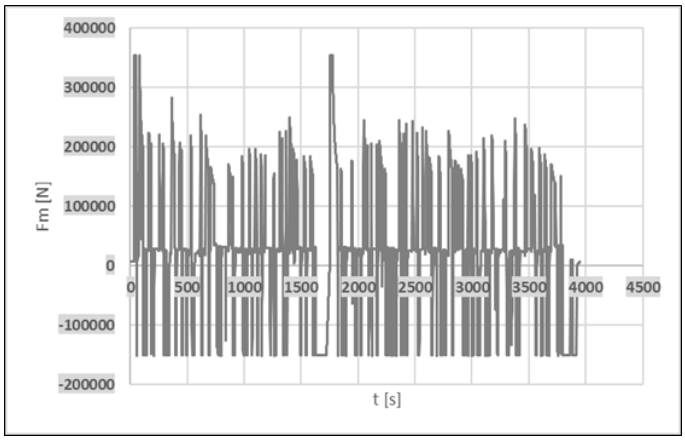

Figure 9 Tractive effort as a function of time for the train of the case study, Campinas – Barra Funda route with PMSM's

Figure 10 presents values of electric current collected as a function of time for the train of the case study, Campinas – Barra Funda route using permanent magnet synchronous motors.

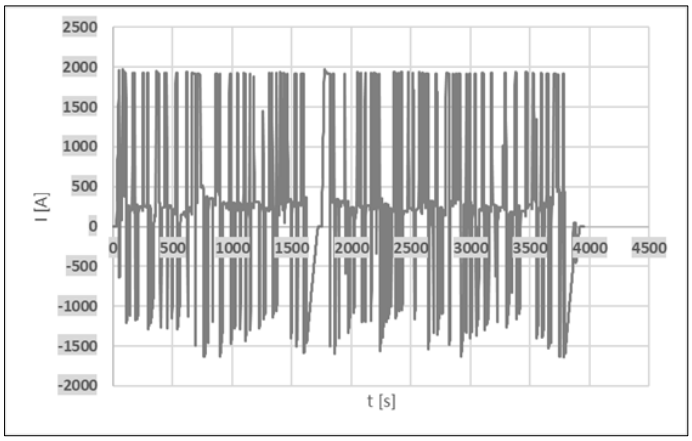

Figure 10 Electric current collected as a function of time for the train of the case study, Campinas – Barra Funda route with PMSM's

In figure 11 is presented the variation of electrical power demanded as a function of time for the train of the case study, Barra Funda - Campinas route using induction motors.

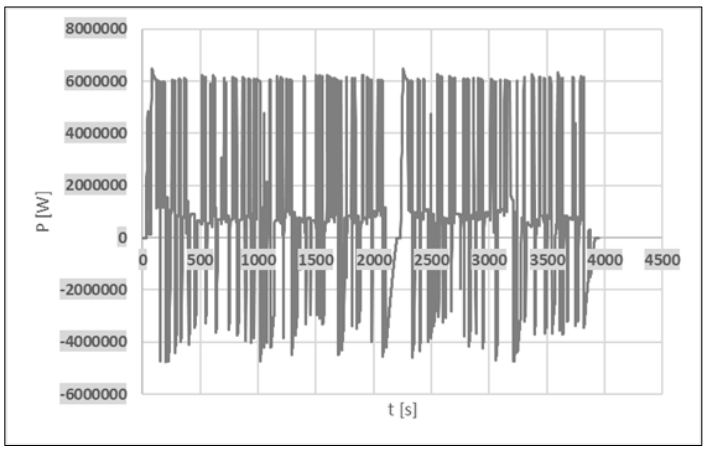

Figure 11 Electrical power demanded as a function of time for the train of the case study, Barra Funda – Campinas route with induction motors

Finally, the variation of electrical power demanded as a function of time for the train of the case study, Barra Funda - Campinas route using PMSM's, is shown in figure 12.

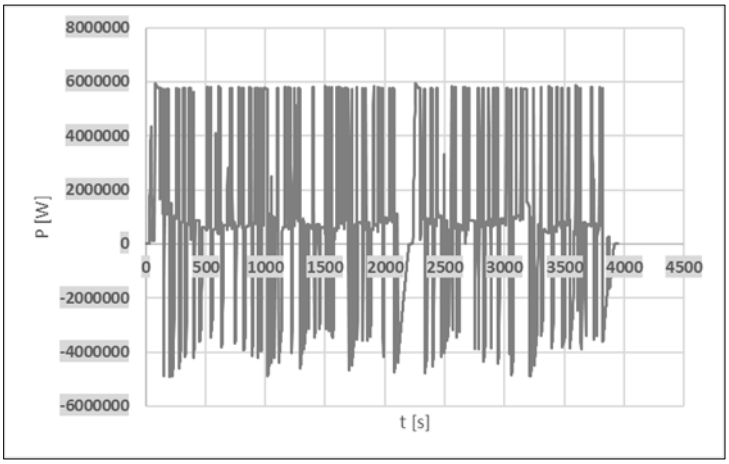

Figure 12 Electrical power demanded as a function of time for the train of the case study, Barra Funda – Campinas route with PMSMs

With numerical integration technique by trapezoidal rule of power curves as a function of time, it is possible to obtain the values of energy consumed by the case study train in the railway sections considered, presented in table 5, for the use of induction machines and permanent magnet synchronous motors, showing the savings achieved with the application of PMSM's.

Table 5 Energy demanded for the train of the case study using induction motors and PMSM's

Motors Type	Energy Demanded - Trip Sections [kWh]
Induction	2294.61
PMSM's	2033.95

Based on the data obtained in table 5, the result is presented that the application of induction motors in the model of regional railroad adopted in the case study resulted in an energy consumption per route 12.81% higher than the with use of permanent magnet synchronous motors, proving the greater efficiency and energy savings provided by PMSM's also in these specific types of railroad and trains.

4. Conclusion

This work presented, initially based on a study of the theoretical literature and conceptualization of railway electric traction drives, a comparative study between induction motors and PMSM's, as traction elements specifically in regional railways, in terms of energy efficiency. The use of the dynamic variables of the railway and train models adopted in the case study, in railway computational simulations, provided data and graphic results that allowed, for the railway section under study, an energy saving of 11.35% per trip of each train, with the replacement of induction motors by PMSM's.

Compliance with ethical standards

Acknowledgments

This research did not receive any specific grant from funding agencies in the public, commercial, or not-for-profit sectors.

References

[1] Allenbach, J.: Electric Traction, Swiss Federal Institute of Technology in Lausanne, 2016, http://www.traction-electrique.ch/documents/Fich1109.pdf, accessed March 2023.

[2] Bossio, J. et al.: Rotor fault diagnosis in permanent magnet synchronous machine using the midpoint voltage of windings, IET Electric Power Applications, vol. 14, no. 2, pp. 256-261, 2020. doi: 10.1049/iet-epa.2019.0428.

[3] Brenna, M. et al.: Electrical Railway Transportation Systems, 1. Ed, Wiley-IEEE Press, 2018, 603p.

[4] Chapman, S.: Electric Machinery Fundamentals, 5. Ed, McGraw-Hill, 2011, 704 p.

[5] Cheng, M. et al.: Cooling System Design and Thermal analysis of a PMSM for Rail Transit, 15th IEEE Conference on Industrial Electronics and Applications (ICIEA), 2020, pp 1912-1915. doi: 10.1109/ICIEA48937.2020.9248320.

[6] Duan, M. Ou, Z. Deng, C.: Analysis of Shaft Voltage in Rotor Permanent Magnet Synchronous Motor System for Traction, 2020 15th IEEE Conference on Industrial Electronics and Applications (ICIEA), 2020, pp. 1908-1911. doi: 10.1109/ICIEA48937.2020.9248127.

[7] Edward, I. Wahsh, S. Badr, M: Analysis of PMSM drives for electric vehicles, 37th SICE Annual Conference, International Session Papers, 1998. pp. 979-984. doi: 10.1109/SICE.1998.742963.

[8] Franko, M. Kuchta, J. Buday, J.: Development and performance investigation of permanent magnet synchronous traction motor, International Symposium on Power Electronics, Electrical Drives, Automation and Motion, Sorrento, 2012, pp. 70-74. doi: 10.1109/SPEEDAM.2012.6264450.

[9] Frenzke. T. Piepenbreier, B.: Position-sensorless control of direct drive permanent magnet synchronous motors for railway traction, 2004 IEEE 35th Annual Power Electronics Specialists Conference, 2004, pp. 1372-1377, Vol.2. doi: 10.1109/PESC.2004.1355623.

[10] Funieru, B. Binder, A.: Thermal design of a permanent magnet motor used for gearless railway traction, 2008 34th Annual Conference of IEEE Industrial Electronics, 2008, pp. 2061-2066. doi: 10.1109/IECON.2008.4758274.

[11] Halder, S. Agarwal, P. Srivastava, S.: Permanent magnet synchronous motor drive with wheel slip control in traction application, 2nd International Conference on Recent Advances in Engineering & Computational Sciences (RAECS), Chandigarh, 2015, pp. 1-4. doi: 10.1109/RAECS.2015.7453402.

[12] Huang, Z. et al.: Design of an interior permanent magnet synchronous traction motor for high-speed railway applications, 6th IET International Conference on Power Electronics, Machines and Drives (PEMD), 2012, pp. 1-6. doi: 10.1049/cp.2012.0253.

[13] Koerner, O. Cai, J. Adam, C.: Permanent magnet motor technology for Velaro high speed train, Zev Rail Rolling Stock, no. 141, 2017, pp. 462-468.

[14] Kondou, K. Matsuoka, K: Permanent magnet synchronous motor control system for railway vehicle traction and its advantages, Proceedings of Power Conversion Conference - PCC '97, 1997, pp. 63-68, vol.1. doi: 10.1109/PCCON.1997.645587.

[15] Parsa, L. Toliyat, H.: Fault-Tolerant Interior-Permanent-Magnet Machines for Hybrid Electric Vehicle Applications, IEEE Transactions on Vehicular Technology, vol. 56, no. 4, pp. 1546-1552, 2007. doi: 10.1109/TVT.2007.896978.

[16] Sandberg, A.: PM motors for railway applications, Grona Taget, Bombardier, 2010, http://www.gronataget.se/upload/PM%20motors%20for%20railway%20applications.pdf, accessed March 2023

[17] Metropolitan Transportation Authority, Public Hearing for the Intercity Train Project - North Axis, São Paulo, Brazil, 2021, http://www.parcerias.sp.gov.br/Parcerias/Projetos/Detalhes/136, accessed March 2023.

[18] Shikata, K. et al.: PMSM propulsion system for Tokyo Metro, 2012 Electrical Systems for Aircraft, Railway and Ship Propulsion, 2012, pp. 1-6. doi: 10.1109/ESARS.2012.6387456.

[19] Vagati, A.: Performance Comparison Between Surface-Mounted and Interior PM Motor Drives for Electric Vehicle Application, IEEE Transactions on Industrial Electronics, vol. 59, no. 2, pp. 803-811, 2012. doi: 10.1109/TIE.2011.2151825.

[20] Xu, Z. et al.: Predictive current control method for dual three-phase PMSM drives with reduced switching frequency and low-computation burden, IET Electric Power Applications, vol. 14, pp. 668-677, 2020. doi: 10.1049/iet-epa.2019.0529

[21] Yu, D. et al.: Design and comparison of interior permanent magnet synchronous traction motors for high-speed railway applications, IEEE Workshop on Electrical Machines Design, Control and Diagnosis, Nottingham, 2017. pp. 58-62. doi: 10.1109/WEMDCD.2017.7947724.